Algal Research 7 (2015) 66–77

Contents lists available at ScienceDirect

Algal Research

journal homepage: www.elsevier.com/locate/algal

Molecular mechanisms for photosynthetic carbon partitioning into storage neutral lipids in *Nannochloropsis oceanica* under nitrogen-depletion conditions

Jing Jia [a,b], Danxiang Han [c,**], Henri G. Gerken [c], Yantao Li [d], Milton Sommerfeld [c], Qiang Hu [e], Jian Xu [a,*]

[a] Single-Cell Center, CAS Key Laboratory of Biofuels and Shandong Key Laboratory of Energy Genetics, Qingdao Institute of BioEnergy and Bioprocess Technology, Chinese Academy of Sciences, Qingdao, Shandong 266101, China
[b] University of Chinese Academy of Sciences, Beijing 100049, China
[c] Laboratory for Algae Research and Biotechnology, Department of Applied Biological Sciences, AZ State University, Mesa, AZ85212, USA
[d] Institute of Marine and Environmental Technology, University of Maryland, Baltimore, MD 21202
[e] Center for Microalgal Biotechnology and Biofuels, Institute of Hydrobiology, Chinese Academy of Sciences, Wuhan, Hubei 430072, China

ARTICLE INFO

Article history:
Received 12 September 2014
Received in revised form 8 November 2014
Accepted 16 November 2014
Available online 17 December 2014

Keywords:
Nannochloropsis
Carbon partitioning
Storage carbohydrates
Lipidomes
Membrane lipids

ABSTRACT

Polysaccharides are a major carbon/energy-reservoir in microalgae, yet their relationship with another form of carbon/energy storage, triacylglycerol (TAG), is poorly understood. Here employing oleaginous microalga *Nannochloropsis oceanica* as a model, we probed the crosstalk between carbohydrate metabolism and TAG accumulation by tracking the temporal dynamics of lipidomes, monosaccharides and polysaccharides and transcripts of selected genes over 14 days under nitrogen-depleted (N−) and nitrogen-replete (N+) conditions. Glucose, galactose and mannitol were the main monosaccharides in IMET1, and laminarin may be the storage polysaccharide that competes for carbon precursors with TAG. Transcriptional expression analysis revealed that the β-1,3-glucan degradation and pyruvate dehydrogenases pathways were the main regulatory components involved in driving carbon flow to TAG synthesis. Furthermore, temporal changes of lipidomes and transcripts of glycerolipid metabolism genes were indicative of possible conversion of membrane lipids to TAG, especially under an early stage of nitrogen deprivation conditions. A carbon partitioning model for *N. oceanica* was proposed, in which β-1,3-glucan metabolism, acetyl–CoA synthesis and membrane lipid turnover/degradation, in addition to *de novo* fatty acid synthesis, all contributed to TAG synthesis.

1. Introduction

Under stress conditions such as nitrogen (N) deprivation, microalgae can store photosynthetically fixed carbon in the form of oils, i.e., energy-dense neutral lipids (e.g., triacylglycerols; TAG), which can be converted to biofuels along with other potential applications [1–3]. However a key biological hurdle for an economically viable microalgal oil industry is the lack of desirable industrial strains capable of high oil productivity in outdoor large-scale cultivation [4,5].

In many microalgae, multiple forms of storage carbon products derived from the photosynthetically fixed carbon can be found (such as water-soluble polysaccharides, starch and TAG [6–8]). As biosynthesis of the multiple forms of storage compounds may require the same carbon precursors (e.g. glucose) and reducing power [9,10], and thus, understanding and tuning the partitioning of carbon precursors into the various forms of carbon storage are of key interest for rational metabolic engineering of industrial microalgal strains for improved oil production.

Polysaccharides such as starch are one abundant form of carbon in many microalgae. For example, we and others showed that the model microalga *Chlamydomonas reinhardtii* can accumulate starch as much as 40% of cell dry weight under high light and N deprivation conditions [11–13]. Moreover, genetically blocking the starch synthesis pathway in *Chlamydomonas* cells led to over 10-fold increase in TAG accumulation [11,13,14]. It was further revealed that the carbon metabolism of the starchless mutant featured an increased carbon flow towards hexose-phosphate by up-regulation of the glyoxylate pathway and gluconeogenesis [15]. In the model diatom *Phaeodactylum tricornutum*, it is not starch but chrysolaminarin that is the main form of storage polysaccharide and can make up 20%–30% of cell dry weight [16], and like starch biosynthesis in *C. reinhardtii*, the chrysolaminarin synthesis pathway competes for carbon with the pathways for lipid biosynthesis [17]. These results suggested that the manipulation of carbohydrate metabolism might potentially enhance TAG production. However, most studies that probed the role of carbohydrates in lipid accumulation have been

* Correspondence to: J. Xu, Single-Cell Center, CAS Key Laboratory of Biofuels and Shandong Key Laboratory of Energy Genetics, Qingdao Institute of BioEnergy and Bioprocess Technology, Chinese Academy of Sciences, Qingdao, Shandong 266101, China.
** Corresponding author.
E-mail addresses: danxianghan@ihb.ac.cn (D. Han), xujian@qibebt.ac.cn (J. Xu).

http://dx.doi.org/10.1016/j.algal.2014.11.005
2211-9264/

conducted in laboratory model organisms such as *C. reinhardtii* and *P. tricornutum* [15,17]. For oleaginous microalgae with demonstrated capability for large-scale cultivation, experimental evidence for the dynamic relationship between carbohydrates and neutral lipids during the oleaginous process has been sparse, largely due to the poor knowledge about identity, profiles and dynamics of storage carbohydrates in these non-model organisms.

Another abundant form of carbon in microalgal cells is membrane lipid, which makes up 5 to 20% of cell dry weight [18–20]. The conversion of membrane lipids into TAG may occur in microalgae, though potential contribution of this pathway to overall TAG biosynthesis has yet to be determined. In *C. reinhardtii*, it was suggested that the acyl moiety of membrane glycerolipids can be transferred to a diacylglycerol molecule by a phospholipid:diacylglycerol acyltransferase (PDAT) to produce TAG, or it can be cleaved by a lipase and then activated to form acyl-CoA for *de novo* TAG biosynthesis [21,22]. In *Nannochloropsis gaditana* [23] and *N. oceanica* [24,25], it was shown that a small amount of accumulated TAG under N-deprivation was postulated to be linked to degradation and recycling of membrane lipids. This was further supported by the up-regulation of the genes encoding *PDAT* and specific lipases during the first 48 hours (h) of N deprivation [24]. However, it is not known whether or how the membrane lipids and TAG homeostasis was sustained beyond such initial phase of TAG accumulation under N deprivation.

Nannochloropsis spp. are a group of unicellular photosynthetic heterokonts distributed widely in sea, fresh and brackish waters. They are of industrial interest due to their ability to grow rapidly, synthesize large amounts of TAGs and high-value polyunsaturated fatty acids (PUFAs) (e.g., eicosapentaenoic acid) and tolerate broad environmental and culture conditions [26,27]. The genomes of several *Nannochloropsis* species have been sequenced [28–33], and the transcriptome and lipidome of one of the species *N. oceanica* IMET1 were simultaneously characterized for the first 48 h of N depletion [24,34]. However, the role of carbohydrates and the link between carbohydrates and TAG in the TAG-accumulating process are not clear. Considering that the cellular content of lipids can reach over 50% of cell dry weight over an extended period of time under N deprivation [25,35], elucidation of longer-term responses beyond the first 48 h of N depletion should be crucial.

In this study, employing oleaginous microalga *N. oceanica* IMET1 as a model, we probed the crosstalk between carbohydrate metabolism and accumulation of TAG, by generating time-course profiles of neutral sugars and glycerolipids in *N. oceanica* IMET1 cells grown under N-replete (N+) and N-depleted (N−) conditions for 14 days, which shed light on carbon partitioning dynamics in *N. oceanica* IMET1. In parallel, transcripts levels of the key genes in glycerolipids and carbohydrate metabolisms were tracked, which further revealed the potential contribution of membrane lipids and storage carbohydrates to TAG biosynthesis. Finally, a carbon partitioning model for *N. oceanica* was proposed. These findings pave the way for understanding and exploiting the links between carbohydrate and lipid metabolisms for enhanced oil production in this and related microalgae.

2. Materials and methods

2.1. Algal strains, culture conditions and nitrate measurements

N. oceanica strain IMET1 was cultured in a modified f/2 medium containing 1000 mg L^{-1} $NaNO_3$ [24]. The final pH was adjusted to 7.8. For the preparation of inoculum, microalgal cultures were grown in nitrogen-replete medium in 1 L columns at 22 °C with 24 h cool white fluorescent illumination (55 μmol m^{-2} s^{-1}) bubbled with 1.5% (w/w) CO_2, with the initial cell density as 3×10^7 cells mL^{-1}. At the log phase (cell density of ~2×10^8 cells mL^{-1}), cells were harvested by centrifugation (3500 *g* at 20 °C for 5 min). The harvested cells were resuspended to 2×10^8 cells mL^{-1} in nitrogen-replete medium (modified f/2 1000 mg L^{-1} $NaNO_3$; N+) or nitrogen-depleted medium (modified f/2 without $NaNO_3$; N−). The cells were cultivated under conditions identical to that of inoculum preparation. The cultures were sampled at 1, 2, 3, 4, 8 and 14 days after the start of nitrogen depletion or repletion. Cells were pelleted by centrifugation (3500 *g* at 20 °C for 5 min). Aliquots for RNA preparation were frozen by liquid nitrogen and then stored at −80 °C, while those for lipidome analysis were washed with water and freeze-dried. Algal culture was centrifuged at 3500 *g* at 20 °C for 5 min and the supernatants were used to measure the nitrate concentration by using a QuikChem 8500 (Lachat Instruments, Loveland, CO, USA) following the manufacturer's instructions.

2.2. Analysis of total lipid, total carbohydrate and total protein contents

Thirty milligrams lyophilized algal powder was loaded to Dionex ASE350 (Thermo Scientific) and extracted by methanol:dimethyl sulfoxide (DMSO) (9:1, v/v) once and by hexane:ethyl ether (1:1, v/v) twice. The extraction temperature and pressure were 125 °C and 1500 psi respectively. The extracts were centrifuged at 1000 *g* for 10 min after being mixed with 15 mL water and then the upper organic layer was transferred to a new labeled vial. The centrifugation and transfer procedure were repeated until the lipid was completely eluted. In the end, the organic layer was evaporated under the protection of nitrogen gas and then freeze-dried overnight. Total lipid content was calculated as net lipid weight divided by net algal biomass weight.

Ten milligrams of lyophilized algal powder was used for the analysis of total carbohydrate content [36]. Briefly the algal powder was incubated with 0.5 mL acetic acid at 80 °C for 20 min and then 10 mL acetone was added, followed by centrifugation at 3500 *g* for 10 min. The supernatant was discarded. The pellet was resuspended in 2.5 mL 4 M trifluoroacetic acid (TFA) and then boiled for 4 h. The suspension was cooled and then centrifuged at 10,000 *g* for 3 minutes. Then 20 μL supernatant was mixed with 900 μL sulfuric acid (15 mL):H_2O (7.5 mL):phenol (0.15 g) and boiled for 20 min prior to reading the optical density at 490 nm (OD_{490}). To quantify total carbohydrate content, glucose was used to establish the standard curve.

Total protein content was determined as previously described [37]. Briefly, 10 mg freeze-dried algal powder was hydrolyzed in 100 μL of 1 M sodium hydroxide (NaOH) and then incubated at water bath at 80 °C for 10 min. Then 900 μL H_2O was added to the hydrolysate to bring the volume to 1 mL. The mixture was centrifuged at 12,000 *g* for 30 min and the supernatant was transferred to a new tube. This extraction procedure was repeated twice, and all the resulted supernatants were pooled together. Then the protein concentration was measured by Bio-Rad Protein assay kit (cat no. 500-0002). Bovine serum albumin (BSA) was used as standard.

2.3. Quantification of intracellular neutral sugars

Freeze-dried biomass (100 mg) was dissolved in 25 mL H_2O, and 10 μL DNase (2 U μL^{-1}) was used to remove DNA. Then the sample was processed in French Pressure to break cell wall. The pressure was set as 20,000 psi and samples were treated for four paths. Efficiency of the disruption was monitored by microscopic observation and centrifugation. Then the ruptured cells were centrifuged at 27,000 *g* at 4 °C for 20 min. The supernatant was boiled at 100 °C for 10 min and then freeze-dried. The resulted samples were resuspended in 5 mL sterilized H_2O and distributed into five aliquots: three were treated with 2 M TFA at 100 °C for 6 h to release glucose in polymeric form, while the remaining two were treated under sterilized H_2O at 100 °C for 6 h. Then the aliquots were evaporated in vacuum under nitrogen gas to remove TFA. The pellet was resuspended in H_2O and the suspension was treated with a 0.22 μm filter. Finally, the suspension was diluted and analyzed with DIONEX ICS-5000 PA10 column using 1 M potassium hydroxide as eluent.

2.4. Lipidome analysis

Ten milligrams freeze-dried microalgal biomass was ground with liquid nitrogen three times, rinsed once with 6 mL chloroform:methanol (2:1, v/v) and then transferred to glass vials for lipid extraction. The samples were incubated at 28 °C for 1 h in a shaker (280 rpm). After the addition of 1.5 mL potassium chloride (0.7%, w/v), the solution was vigorously mixed to remove protein, centrifuged at 1000 *g* for 5 min at room temperature, and then the lower organic phase (total lipid was in this phase) was transferred to a new glass vial using Pasteur pipette. Then the solvent was evaporated in vacuum under N_2 flux. The extracted lipids were stored at −20 °C.

Mass spectrometry analysis was performed with an Agilent 6460 triple quadrupole liquid chromatography/mass spectrometer equipped with an electrospray ion source (Agilent) according to the method we previously described [22,24]. Internal standards and calibrants used in this study were listed in Table S1.

2.5. Absolute quantification of transcripts in a time-series

Harvested *N. oceanica* IMET1 cell pellets were pulverized in a mortar with liquid nitrogen and the powder was transferred to a tube containing TRIzol (Invitrogen). Total RNA isolation was performed as previously described [38]. High salt solution (0.8 M sodium citrate and 1.2 M sodium chloride) was used to remove polysaccharides. The integrity of the purified total RNA was assessed using 1.2% agarose gel electrophoresis and Agilent 2100 Bioanalyzer. Total RNA quantity was measured by NanoDrop spectrophotometer.

For real-time RT-PCR analysis, first strand cDNA synthesis was carried out using a Taqman Reverse Transcription system (Applied Biosystems). Each 20 μL reaction volume consists of 250 ng total RNA. In controls, the reverse transcriptase was replaced by water to detect contamination from genomic DNA. Real-time PCR was performed on an ABI Prism 7500 (Applied Biosystems) as previously described [38]. The relative abundance of β-actin was also determined (Fig. S1) and used as the internal standard. Primer sequences used are listed in the Table S2.

2.6. Fluorescence microscopy

Neutral lipid accumulation was observed by fluorescence microscopy. Cells were sampled every 24 h. Aliquots of cells were diluted to a density of 1×10^8 cells mL^{-1} and then treated with 10% DMSO [39] and stained for 10 min with 50 μM BODIPY 493/503 (Molecular Probes, Invitrogen Corporation). Images were acquired using an Olympus BX51 microscope. Chlorophyll autofluorescence was detected using a 660/50 band-pass optical filter, and BODIPY 493/503 fluorescence was detected using a 525/50 band-pass filter.

2.7. Determination of fatty acid methyl esters (FAMEs) by gas chromatography with flame ionization detector (GC-FID)

Total lipid was extracted by DIONEX ASE 350 and transesterified as described previously [40,41]. Briefly, 25 μL 10 mg mL^{-1} methyl tridecanoate (C13Me), 200 μL chloroform:methanol (2:1, v/v) and 300 μL 5% (v/v) HCl:methanol were added to 5–10 mg lipid extracts and was transesterified in tightly sealed vials at 85 °C for 1 h. Fatty acid methyl esters (FAMEs) were extracted in 1 mL hexane at room temperature for 1 h. Then the extracted FAMEs with pentadecane as internal standard was analyzed directly by GC-FID using Agilent 7890A gas chromatography with a J&W 122-7032 column. FAMEs were quantified via a standard C8-C24 FAMEs mix (Sigma-Aldrich). C13Me was used as recovery standard.

3. Results

3.1. Dynamics of carbohydrates, lipids and proteins in N. oceanica IMET1 cells during 14 days under N deprivation

3.1.1. Growth kinetics of N. oceanica IMET1 during a 14-day cultivation under N deprivation

The growth of *N. oceanica* IMET1 cultivated in N− or N+ medium was monitored for 14 days (Fig. 1A). During the first four days, the growth rates were comparable between the two treatments. After Day 4, the cell number under N− remained stable until Day 12 and declined afterwards, while that under N+ cell growth continued until Day 11, after which the cells underwent a trend similar to that occurred under N− conditions (Fig. 1A). Taken together, these results indicated that intracellular N reservoir was able to sustain 3–4 days of growth when N was depleted from the culture medium.

To trace TAG accumulation, IMET1 cells were stained with BODIPY 490/503 [39] to visualize lipid bodies (LB) (Fig. 1B). Under N−, the number of LB increased until Day 4, after which it remained more or less unchanged but the size of existing LB increased considerably. A tangible decrease in the LB number was observed after Day 8, probably resulted from fusion of LB. Concurrent with neutral lipid accumulation, chlorophyll *a* autofluorescence in the N− cells attenuated over time, suggesting breakdown of photosynthetic complexes. Under N+, both neutral lipid and chlorophyll *a* fluorescence remained relatively stable during the first 6 days, and after Day 6, the size of LB slightly increased after Day 6 (due to the depletion of N then), which was accompanied by a decrease in chlorophyll *a* autofluorescence.

3.1.2. Changes in total carbohydrate, lipid and protein contents under N deprivation

Photosynthetically fixed carbon can be diverted into multiple pathways for synthesis of major macromolecules like carbohydrates, lipids and proteins [42]. As N is an essential component of proteins and many glycerolipids (e.g. phosphatidylcholine (PC), diacylglycero-4′-O-(N,N,N-trimethyl)-homoserine (DGTS), phosphatidylserine (PS) and phosphotidylethanolamine (PE)) [43,44], profound changes in total carbohydrates, lipids and proteins may occur when N is limited or depleted from the culture medium. Our biochemical analyses showed that the cellular carbohydrate content increased from 5.8% to 17.9% (by dry weight, DW) during the first 4 days and steadily increased to 19.1% on Day 14 under N− (Fig. 1C). Under N+, the cellular carbohydrate content slightly increased during the first 8 days, followed by an increase to 17.4% (by DW) when N in the medium was exhausted. Similar to the kinetics of total carbohydrates, under N−, the content of total lipids increased from 22.0% to 46.3% on Day 8 and then reached 50.5% on Day 14; under N+, the lipid content was ca. 25.6% and increased to 34.0% on Day 7 when N was exhausted from the medium (Fig. 1C). In contrast to total lipids and carbohydrates, the cellular protein content decreased rapidly after the onset of N deprivation and reduced from 38.0% to 9.5% (i.e. 3-fold decrease) over 14 days under N− (Fig. 1C); yet under N+, the protein content decreased from 40% to 22% during the same period of time. After the exhaustion of media N under the N+ condition, total carbohydrate, total lipid and total protein levels all exhibited a lag of two days relative to those under the N− condition. This two-day lag could have been caused by the difference in cellular state at the onset of nitrogen exhaustion between the two culture conditions (the stationary phase under N+ versus the exponential phase under N−).

3.1.3. Change of neutral sugar profiles in response to long-term N deprivation

To identify the major storage carbohydrate in IMET1, the sugar molecules in both monosaccharide and polysaccharide forms were determined and then the absolute contents were quantified by ion chromatography. It revealed that glucose, mannitol and galactose were the major neutral monosaccharides under both N+ and N− conditions

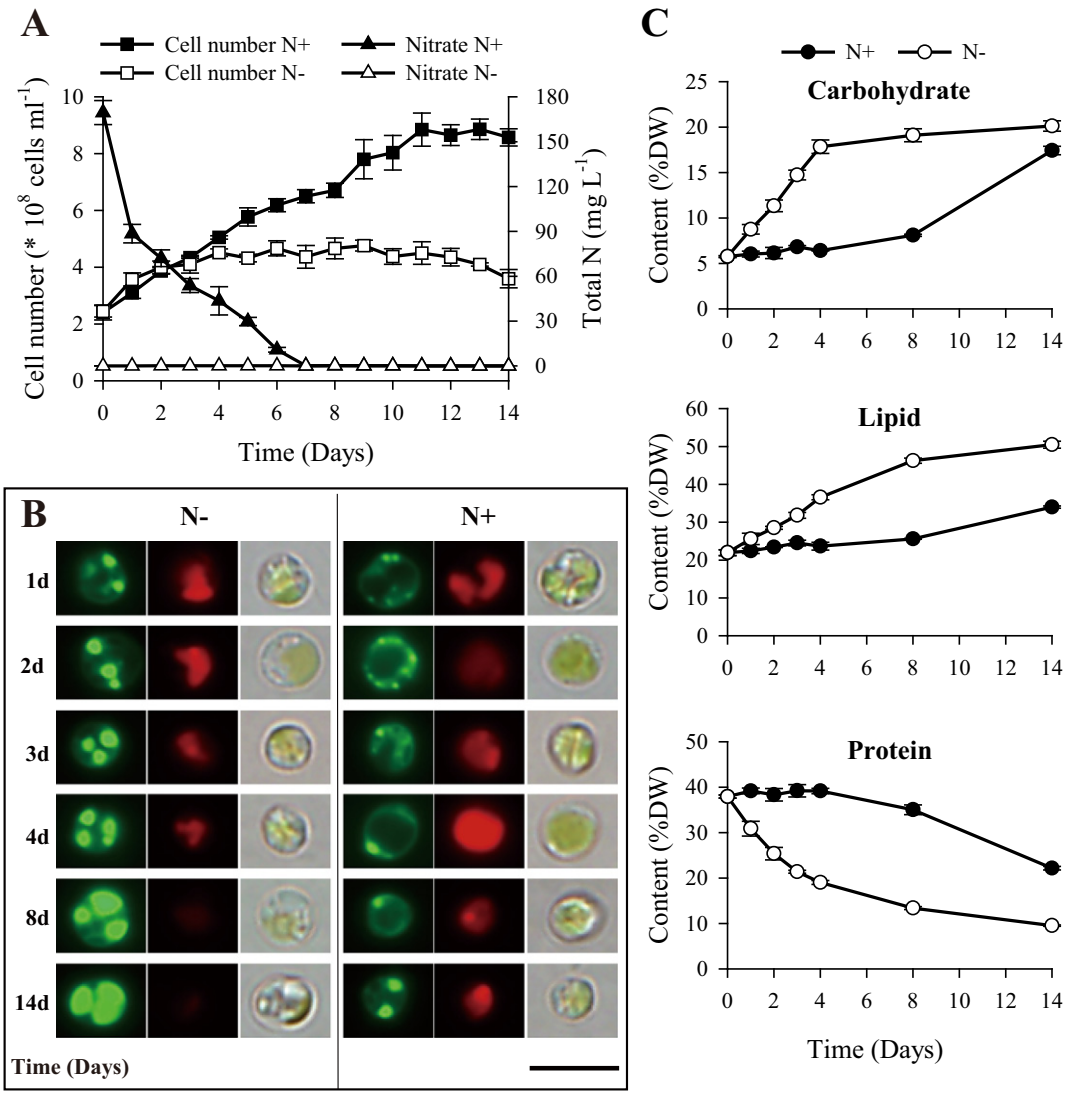

Fig. 1. Growth, nitrogen consumption and biochemical compositions of *Nannochloropsis oceanica* IMET1 under nitrogen-replete (N+) and nitrogen-depleted (N−) conditions. (A) Growth and nitrogen consumption. (B) Contents of total carbohydrate, total lipid and total protein. In (A) and (B), each data point is the average of four biological replicates and error bars represent standard deviation (SD). (C) Microscopic images of IMET1 cells. BODIPY fluorescence: green; Chlorophyll autofluorescence: red. Bar = 5 μm.

(Fig. 2). Glucose was equally distributed into the monomeric and polymeric forms under both N+ and N− conditions. Distinct from glucose, most (80%) of mannitol were in the monomeric form, whereas polymeric galactose was predominant. In addition, trace amounts of fucose, glucosamine and ribose were detected in the polymeric form, while small amounts of rhamnose and mannose were present in both monomeric and polymeric fractions.

Under N−, free glucose increased by 2-fold (from 1.89% to 3.84% DW) during Day 1 and peaked (6.74% DW) on Day 14. However from Day 1 to Day 8 the polysaccharides containing glucose increased from 1.63% to 7.87% under N−, and then slightly declined to 6.28% on Day 14. It was speculated that the increase of free glucose from Day 8 to Day 14 was due to the hydrolysis of polymeric glucose (Fig. 2). Under N+, free glucose varied to a small extent while polymeric glucose decreased by ca. 30%, at the exponential growth phase (Days 0–6), and then both forms dramatically increased after Day 7 when N was exhausted from the growth medium.

Distinct from glucose, under N+, free and polymeric mannitol varied between 4.4 and 6.7% and between 0.9 and 2.0% of DW, respectively. A transient increase in the two forms (8.32% and 3.32% of DW for free and polymeric mannitol, respectively) occurred on Day 2 under N−. Free mannitol decreased to 4.85% (DW) on Day 3 and remained more or less constant thereafter while the polymeric form gradually decreased to 0.9% DW on Day 14.

Under N+, the concentration of free and polymeric galactose was relatively low and oscillated within the range of 0.34–0.53% and 1.22–1.67% of DW in the first 8 days, respectively. After then both forms declined due to the exhaustion of N source. Free galactose dramatically decreased to an undetectable level during the first 2 days under N−, whereas polymeric galactose slightly increased from 1.52% to 1.82% (DW) on Day 3 and then gradually decreased to 0.3% thereafter.

3.2. De novo TAG biosynthesis vs. membrane conversion: insights from lipidome analysis

In addition to polysaccharides, another abundant form of carbon in microalgal cells is membrane lipid, which is mainly composed of membrane glycerolipids. A total of nine glycerolipid classes including 76 molecular species were identified in *N. oceanica* IMET1 and their changes over the first 96 h of N deprivation were determined [24]. In this study, the basal level of glycerolipids in IMET1 was 8.3% of DW under N+, which increased to 44.2% of DW over 14 days under N−

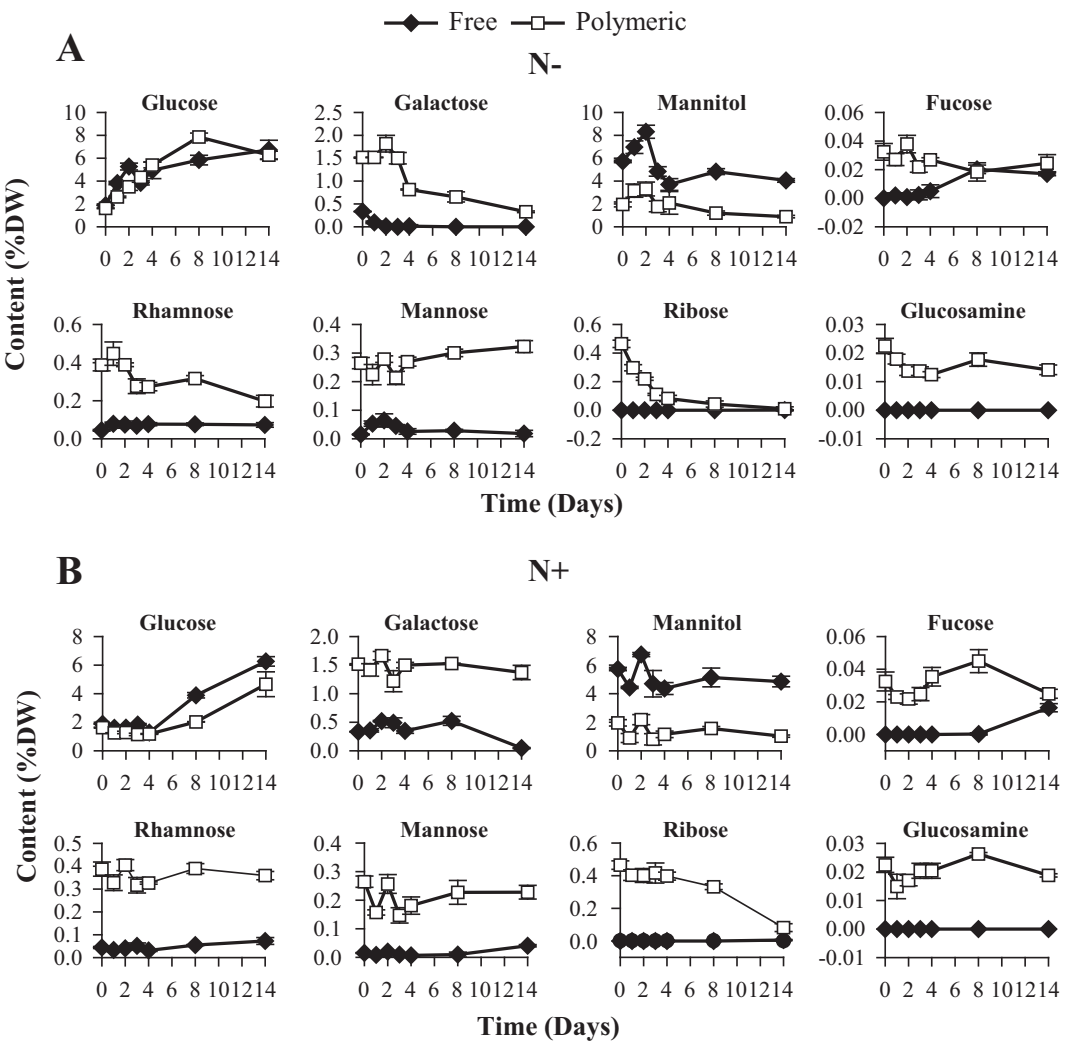

Fig. 2. Neutral sugar profile for *Nannochloropsis oceanica* IMET1 under N− (A) and N+ (B). Filled square line represents sugars in free form while empty square line represents those in polymeric form. Each data point is the average of three biological replicates and error bars represent SD.

(Fig. 3A), 90% of which was TAG (Fig. 3B). Temporal variation of the content of all the 76 glycerolipid species over the 14-day cultivation was also tracked (Fig. 4; Table S3). Concomitant with accumulation of TAG, the total content of membrane glycerolipids (including monogalactosyldiacylglycerol (MGDG), digalactosyldiacylglycerol (DGDG), sulfoquinovosyl diacylglycerols (SQDG), phosphatidylglycerol (PG), PE, phosphatidylinositol (PI), PC and DGTS) decreased from 7.9% to 4.2% of DW after 14 days under N−. Among the membrane glycerolipids, MGDG and PG showed the greatest decline by 71 and 90% over 14 days, respectively (Fig. 3C and D). SQDG, PC, DGTS and PI decreased moderately after Day 2 or 3 under N− (Fig. 3E, F, G and H). In contrast, a two-fold increase in DGDG was observed over 2 days under N deprivation, followed by a gradual decrease to the basal level of 5.0% (Fig. 3I). The only group of glycerolipids not susceptible to N deprivation was PE, a minor class of glycerolipids that remained essentially unchanged under the given experimental conditions (Fig. 3J).

Among the 30 TAG species detected in IMET1, 48:1 (16:0/16:1/16:0), 48:2 (16:1/16:0/16:1), 50:1 (16:0/16:0/18:1), 46:1 (14:0/16:0/16:1) and 50:2 (16:0/16:1/18:1) were the major ones, together accounting for over 60% and 80% of the total TAG under N− and N+, respectively (Fig. S2). A number of TAG species containing various polyunsaturated fatty acids (PUFAs) were identified as minor molecular species (Fig. S2). In the TAG pool, EPA was the most abundant PUFA (Fig. S3). The accumulation of EPA in TAG under N− was correlated with the degradation of several molecular species of EPA-containing membrane glycerolipids (i.e., DGTS (16:1/20:5), DGTS (20:4/20:5), PG (16:0/20:5) and MGDG (20:5/20:5)) (Figs. 4 and 5), suggesting that EPA in TAG was derived from EPA-containing membrane glycerolipids. Several other PUFAs (i.e., C18:2, C18:3 and C20:4)-containing TAG were also increased over the 14 days under N− (Fig. S3).

In contrast to PUFA-containing TAG, the TAG molecules with one or more saturated fatty acid C16:0 or mono-unsaturated fatty acid C18:1 were more likely produced via a *de novo* fatty-acid/TAG biosynthesis pathway than from the membrane conversion. As an evidence, TAG-associated C16:0 increased by 812 μmol g^{-1} DW over the first 8 days under N−, while at the same time C16:0 in membrane lipids decreased by 26 μmol g^{-1} DW, which was only 3% of those incorporated into newly synthesized TAG (Fig. S3; Table S4). Similarly, the major TAG species that contained C18:1 were most likely synthesized via the *de novo* biosynthesis pathway, as under N− C18:1 associated with membrane lipids didn't decrease, but slightly increased. Similar results were obtained by GC-FID analysis of FAMEs (Table S5).

3.3. Transcriptional response of key pathways in carbon partitioning to nitrogen deprivation over 14 days

To gain mechanistic insights into the conversion between membrane lipids/storage carbohydrates and TAG, genes involved in *de novo*, alternative TAG synthesis pathway, and carbohydrate metabolism pathways were measured by absolute quantification real-time PCR. We

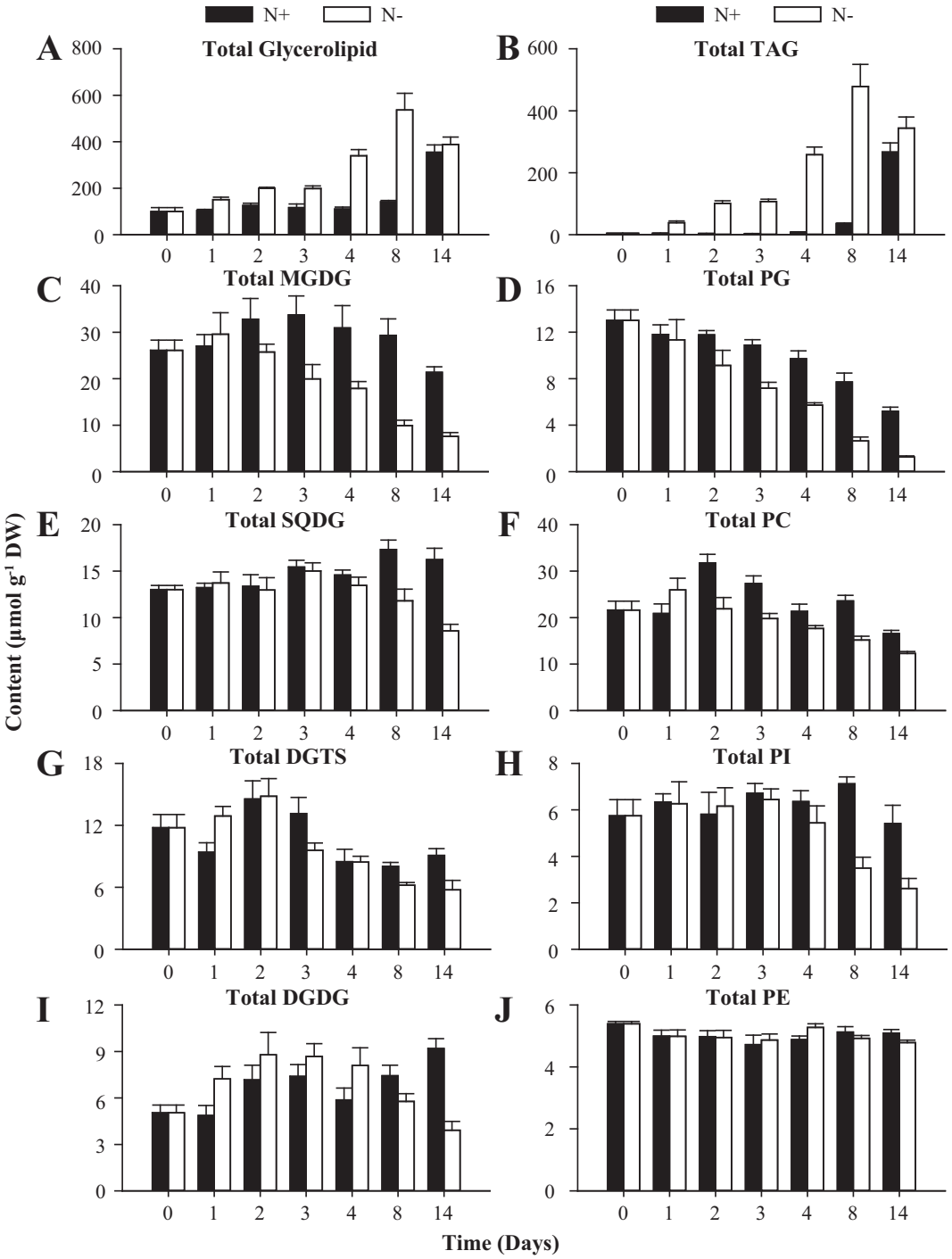

Fig. 3. Cellular content of total glycerolipid (A) and nine major glycerolipid classes, TAG (B), MGDG (C), PG (D), SQDG (E), PC (F), DGTS (G), PI (H), DGDG (I) and PE (J) in *Nannochloropsis oceanica* IMET1 under N− and N+. Each data point is the average of three biological replicates and error bars represent SD.

previously reported that the Kennedy pathway genes were moderately up-regulated during the first 48 h after the onset of N deprivation, particularly for the genes encoding diacylglycerol acyltransferase (DGAT) [24]. A total of 13 DGATs genes (two *DGAT1* and 11 *DGAT2*) were uncovered in *N. oceanica* IMET1 genome [33]. Among them, *DGAT 2A* and *DGAT 2C*, which encode putative cytosolic and plastidic DGAT isoforms, respectively, exhibited higher fold-changes in transcript than the other *DGAT2s* over the first 48 h under N deprivation [24] and thus were selected for gene expression analysis in this study. It revealed that the up-regulation of *DGAT2A* continued until Day 4 under N−; thereafter its expression gradually decreased to a level higher than that under N+ conditions until Day 14 (Fig. 6A). Different from its cytosolic isoform, the expression of plastidic *DGAT2C* [24] peaked on Day 1 and then dropped to a basal level on Day 3 and stayed stable thereafter under N− (Fig. 6A).

The transcript level of *PDAT* peaked on Day 2 under N−, with the high expression level lasting for two days and then declined to the basal level from Day 4 through Day 8. In *C. reinhardtii*, PDAT can utilize glycerophospholipids and galactolipids as acyl donors for TAG biosynthesis [22]. To probe whether PDAT-mediated membrane lipid conversion was transcriptionally coupled with *de novo* membrane lipid biosynthesis, we examined the effect of N deprivation on the genes responsible for biosynthesis of the major phospholipids (PC and PI) and galactolipids (MGDG and DGDG), the possible substrates of PDAT. The

single-copy MGDG synthase gene *MGD* was significantly down-regulated from Day 2 through Day 4, and then remained at the low level for the remaining 10 days (Fig. 6A). Distinct from *MGD*, the DGDG synthase gene *DGD* exhibited little changes during the 14 days

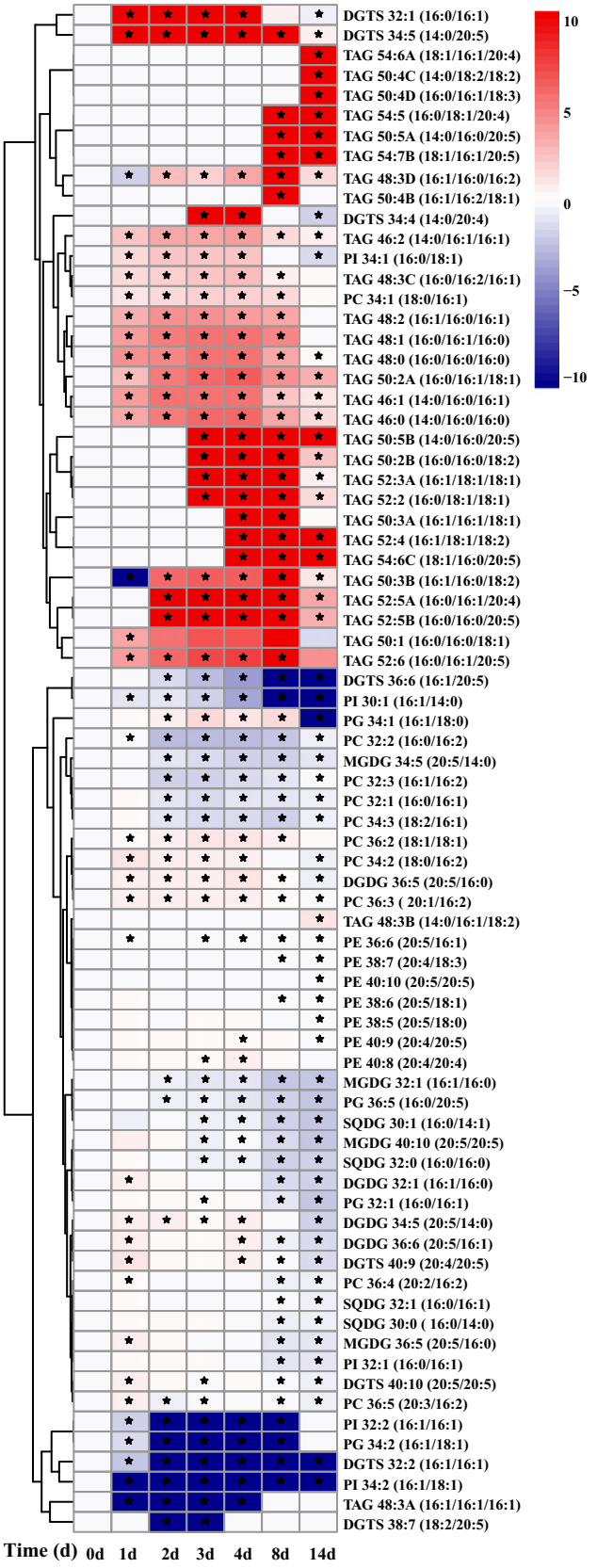

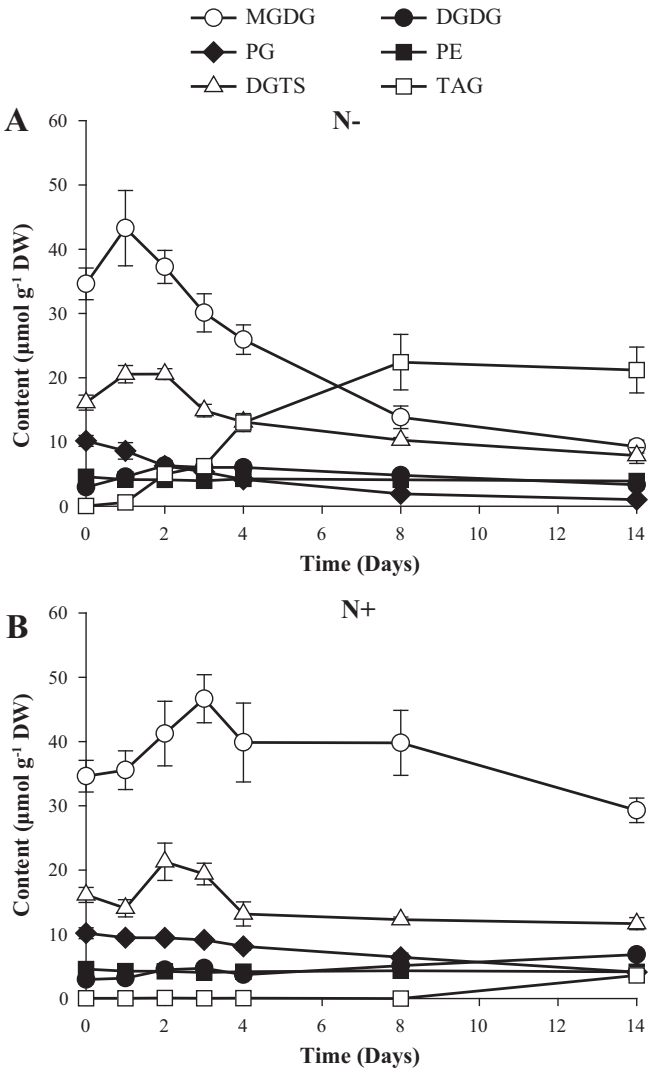

Fig. 5. Variation of EPA content in each of the glycerolipid classes under N− (A) and N+ (B). Values are presented as means ± SD (n = 4–6).

under N− (Fig. 6A). The gene encoding CDP-choline phosphotransferase (CPT), which catalyzes the last committed step of PC biosynthesis, was not responsive to N deprivation during the first 8 days under N−, and then slightly down-regulated on Day 14 (Fig. 6A). Similar to *CPT*, the genes encoding CDP-DAG synthase (CDS) and phosphatidylinositol synthase (PIS), the two enzymes responsible for PI biosynthesis, were down-regulated after the first 8 days under N− (Fig. 6A).

In higher plants, lipases can liberate fatty acids from membrane lipids for TAG biosynthesis [21,45,46]. Transcriptional expression of several lipase genes was significantly up-regulated in *C. reinhardtii* and *N. oceanica* under N depletion [24,34]. In IMET1, the transcript level of diacylglycerol (DAG) lipase alpha gene (*LIPa*) peaked on Day 2 under N− and then declined to the basal level (Fig. 6B). A putative lysophospholipase gene (*LPL*) was induced by N− and its transcripts peaked with >4-fold increase on Day 4 (Fig. 6B). Another putative lipase

Fig. 4. Heat map that illustrates variation of the cellular content of the 76 major glycerolipid species over 14 days in response to nitrogen depletion. Fold change of the lipid content was calculated as $\log_2$(lc(Tx, N−) / lc (Tx, N+)) (lc = content of lipid species, Tx = time point). The value of $\log_2$ (N−/N+) was set as 0 for the species undetectable under both modes, as 10 for species undetectable only under N+, and as −10 for species undetectable only under N−. Significant differences ($P \leq 0.01$) between N− and N+ are indicated with an asterisk. Acyl chains of glycerolipid species are shown as "carbon number: number of double bonds". Values represent means ± SD (n = 4–6). Time refers to the duration (in days) after the onset of N+ or N− conditions.

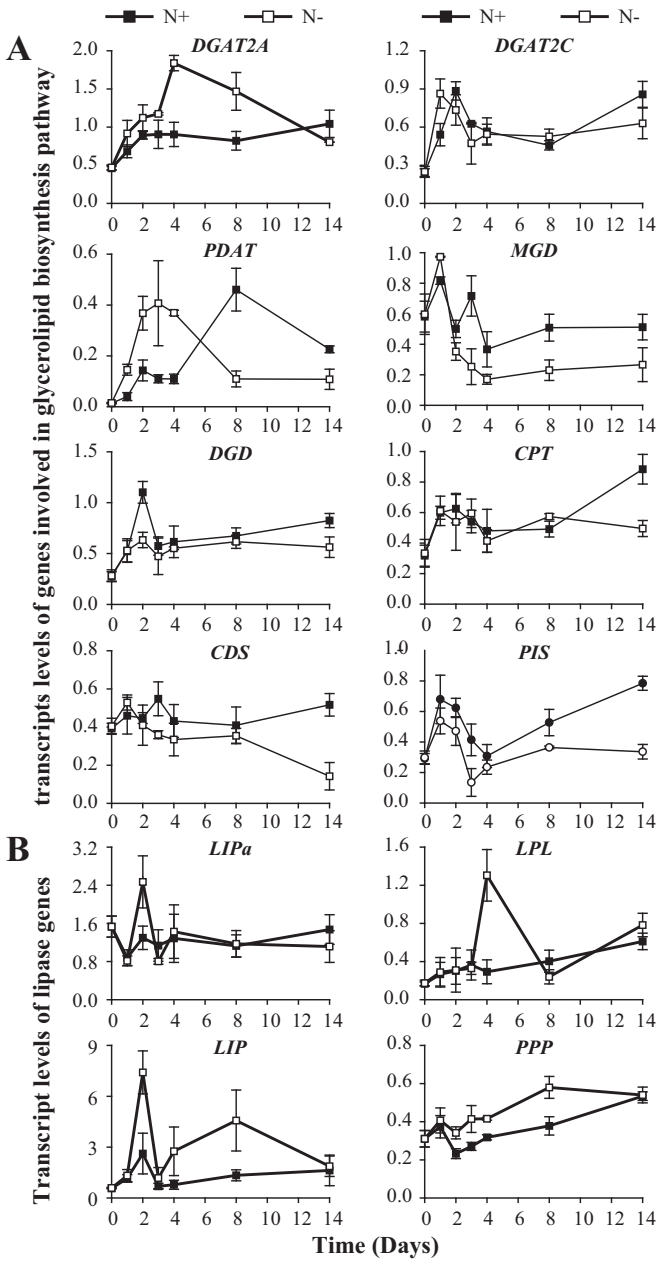

Fig. 6. Transcript dynamics of glycerolipid synthesis and degradation genes under N+ and N−. Transcript abundance was normalized to β-actin gene. Each data point is the average of four to six replicates and error bars represent SD.

gene (*LIP*) showed dual up-regulation in response to N starvation, i.e., a 2-fold increase in transcript occurred on Day 2 and then a 3-fold increase on Day 8 (Fig. 6B). A putative patatin-like phospholipase gene (*PPP*) was progressively up-regulated over 8 days under N− (Fig. 6B).

In addition, three sets of genes in carbohydrate metabolism that potentially supply sugar precursors for TAG synthesis were tracked (Fig. 7). Among the five putative β-glucan synthesis enzymes identified in IMET1, phosphoglucomutase (*PGM*) and UDP-sugar pyrophosphorylase (*UPP*) were induced in the early stage (Day 3) of N deprivation, whereas 1,3-β-glucan synthase (*BS*) was up-regulated on Day 8. Beta-1,3-glucosyltransferase (*BGT*) was the only gene showing up-regulation by two-fold at two time-points under N−, one occurred on Day 1 and the other on Day 8 (Fig. 7A).

It was postulated that β-1,3-glucan was degraded into glucose, which was then converted to pyruvate [24]. The latter was then converted to acetyl–CoA by a pyruvate dehydrogenase [47]. Thus, the five β-1,3-glucan degradation genes (including one glucosyl hydrolase, *GH*; two endoglucanases, *EG* and *EGA*; and two β-glucosidases, *bGS* and *bGSG*) and five genes encoding subunits of pyruvate dehydrogenase (PDH) were tracked (Fig. 7B and C). Only *EGA* increased by 4-fold two days after the onset of N deprivation, and no change in transcript was observed for the other β-glucan degradation-related genes. Among the five *PDH* genes, *PDH1*, *PDH3*, and *PDH4* showed progressive up-regulation over 14 days under N− (Fig. 7C), indicating that production of acetyl–CoA from pyruvate is a key step of transcriptional regulation for TAG accumulation during long-term N deprivation.

3.4. A model of photosynthetic carbon partitioning towards TAG in *N. oceanica*

Dynamics of storage carbohydrates and membrane lipids over 14 days of N-deprivation induced oil production, together with our recently published time-series transcriptome and genome sequence of this organism [24,33], allow reconstruction of a molecular model for photosynthetic carbon partitioning in *N. oceanica* (Fig. 8).

Conversion between storage carbohydrates and TAG can be reflected by changes in β-1,3-glucan to free glucose ratio: its increase implied more carbon partitioned to storage carbohydrates while its decreaseis indicative of redirecting of carbon flux from carbohydrate to TAG synthesis via the glycolysis pathway. The homeostasis of β-1,3-glucans is regulated by their biosynthesis and degradation. Only one single-copy gene for each of the three key biosynthetic enzymes (UPP, BGT and BS) of β-1,3-glucan while multi-copy genes for their degrading enzymes (5 genes for EG/EGA, 10 genes for bGS/bGSG and 13 genes for GH) present in IMET1 genome (Table S6). Such enrichment of β-1,3-glucan degradation genes might suggest an ability of IMET1 to rapidly utilize storage carbohydrate for other cellular metabolisms. To determine possible subcellular localization of β-1,3-glucan synthesis, HECTAR, SignalP, ChloroP and Mitoprot were used [24,33,48–51]. The result indicates that majority of genes involved in β-1,3-glucan metabolism are located in cytosol other than chloroplast and mitochondria (Table S6). As the amount of accumulated β-1,3-glucan accounted for 5%–8% of cell dry weight, which equals to one fourth of total TAG (Figs. 2A and 3B), redirection of carbon flow from β-1,3-glucan to TAG by manipulating the β-1,3-glucan biosynthetic or degrading pathways should enhance TAG productivity.

Conversion between membrane lipids and TAG occurred when N was depleted for IMET1 cells. Membrane lipids are essential components for vividly growing cells, yet under N− they are converted to TAG by PDAT and lipases. A single-copy *PDAT* gene and 30 lipases genes were identified in IMET1. Subcellular localization analysis revealed that *PDAT* and 14 lipase genes are located in neither mitochondria nor chloroplast (Table S6); their probable localization in cytoplasm may suggest the crucial contribution of cytoplasm in conversion of membrane lipids to TAG. After 14 days under N−, total phospholipids and galactolipids decreased by 54% and 62% respectively. Intriguingly, the decrease of phospholipids content, starting on Day 3, preceded that of galactolipids by 24 h, suggesting that their conversion to TAG follows a certain temporal order.

4. Discussion

4.1. Features of biosynthesis and degradation of storage carbohydrates in IMET1

Unlike green microalgae and cyanobacteria that employ α-1,4-glucan-based starch and glycogen, respectively, as a carbon storage, heterokonts like *N. oceanica* produce chrysolaminarin or laminarin as a carbon reserve which is made of β-1,3-glucans with occasional β-1,6-linked branches [6,10]. Laminarin and chrysolaminarin are distinguished by the monosaccharides at the terminus of glucans:

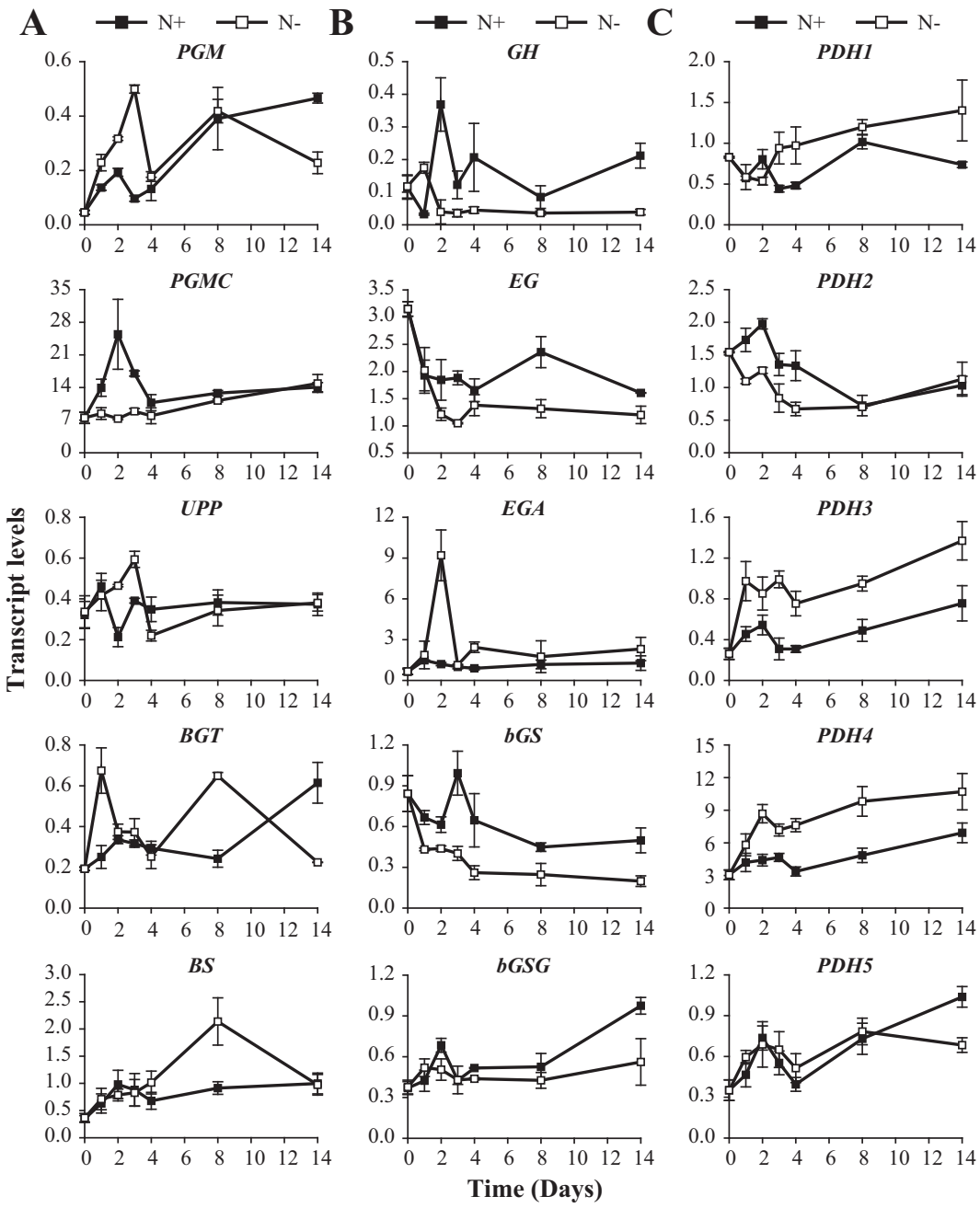

Fig. 7. Transcript dynamics of genes involved in β-glucan synthesis (A), β-glucan degradation (B), pyruvate decarboxylation (C) under N+ and N−. Transcript abundance was normalized to β-actin gene. Each data point is the average of four to six replicates and error bars represent SD.

laminarin is a mixture of two molecular species, with the major one terminated with a 1-linked mannitol residue (M-chains) and the minor one terminated with reducing glucose residues (G-chains), whereas chrysolaminarin is solely composed of G-chains of β-1,3-glucans that does not contain mannitol [6,10]. Although the β-1,3-glucan synthesis genes were predicted in *Nannochloropsis* genomes [33], direct biochemical evidence for the presence of either chrysolaminarin or laminarin has been lacking. Our analysis revealed that it was laminarin but not chrysolaminarin that may be the storage carbohydrate in IMET1 and that was accumulated under N−.

Mannitol, the minor component of laminarin, was synthesized via mannitol cycle in IMET1 (based on analysis of the genome and transcriptomes of this organism; [24,33]). Mannitol synthesis in heterokonts was proposed to involve reduction of fructose-6-P to the intermediate mannitol-1-phosphate by a mannitol-1-phosphate dehydrogenase (M1PDH), and then sequential dephosphorylation of mannitol-1-phosphate. Although this pathway resembles the one identified in fungi [52], in the brown algae the dephosphorylation step was catalyzed by a haloacid dehalogenase (HAD)-like enzyme [10,53], instead of a mannitol-1-phosphatase (M1Pase) found in fungi [52]. In IMET1 one M1PDH gene and three HAD genes were present but an M1Pase gene was absent in the genome. The synthesized free mannitol can be reverted to fructose-6-P by mannitol-2-dehydrogenase (M2DH) and fructokinase, or added to the terminus of β-1,3-glucan chains via a yet unknown pathway.

Beta-1,3-glucan, another component of laminarin, also exhibits distinct features in IMET1. Synthesis and degradation of β-1,3-glucan in IMET1 highly resemble those in brown algae, which also synthesized

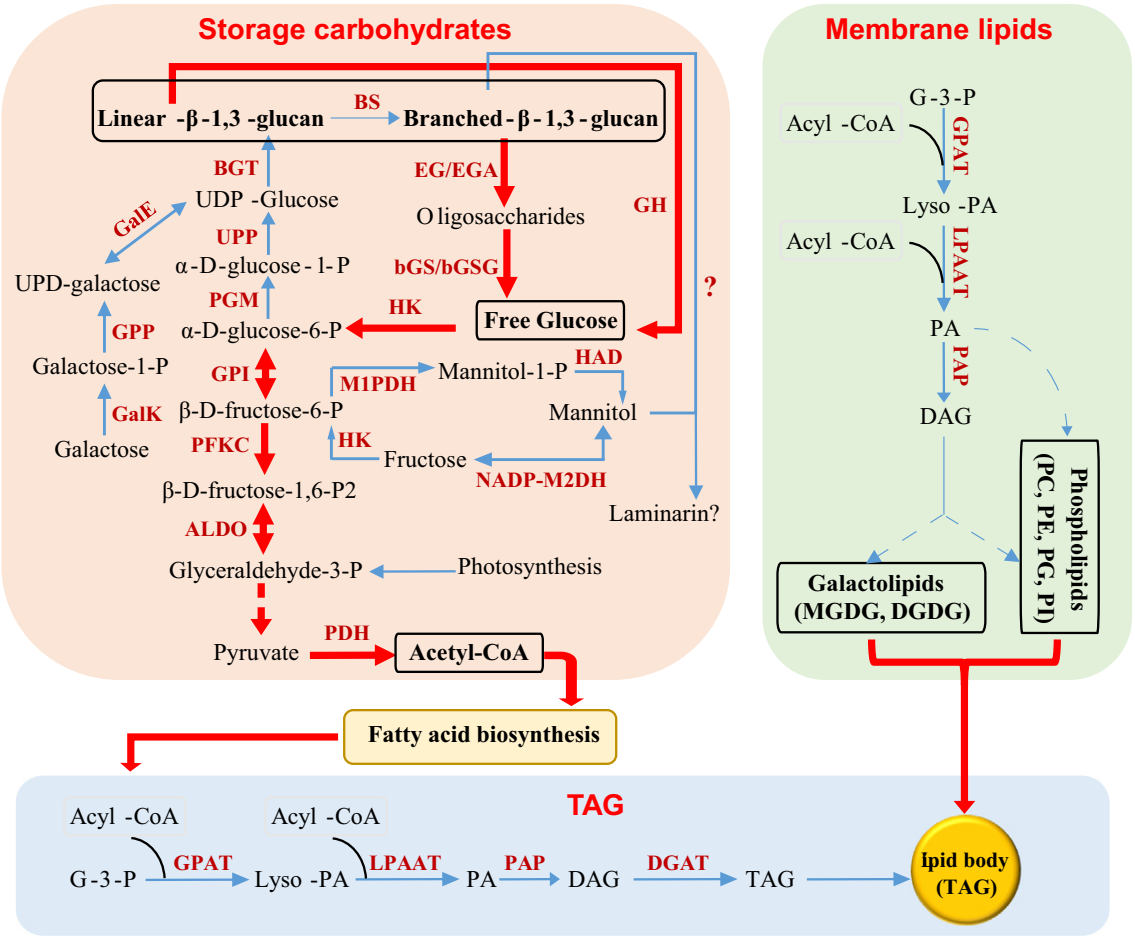

Fig. 8. A model of photosynthetic carbon partitioning towards TAG in *Nannochloropsis oceanica*. Key chemical compounds were illustrated in the black box. The solid line arrows represent one-step reaction while dashed ones represent multi-step reaction. The red arrows illustrate the two main carbon reallocation routes in IMET1.

laminarin as its carbon storage form [10,33]. The genes encoding endo-1,3-β-glucanases, exo-1,3-β-glucanases and β-glucosidases were identified in IMET1, and each gene had multiple copies [33]. These genes may work complementarily in a way similar to that in *Phaeodactylum tricornutum* [54]. The high dose of β-glucosidases genes (10 copies) may account for the continuous increment of free glucose in IMET1 over the 14-days under N deprivation stress. Based on the results of this and other studies [24,33], a carbohydrate metabolic network in *N. oceanica* IMET1 was reconstructed (Fig. 8).

4.2. Implication of the carbon partitioning model in microalgal feedstock development

In higher plants, carbon partitioning is a highly regulated process that involves the transportation of photosynthates as well as coordination of enzyme activities across various organs [55–57]. Photosynthesis and carbon fixation take places in leaves, with sucrose and starch as preliminary sinks [58]. Carbon compounds, which are sucrose for majority of higher plants, are then transported from source tissues (i.e., mature leaves) to sink tissues (roots and other nonphotosynthetic organs) by phloem. Transporters/channels of sucrose, K^+ and water, as well as H^+-ATPase, all play crucial roles in regulating the transport of sucrose in the phloem [59]. In sink tissues, the sucrose is then broken down in cytosol and then converted to starch in amyloplasts [60,61]. Unlike higher plants, sucrose has not been found as a major sink for carbon in microalgae [59,62]. Moreover, for microalgae, carbon fixation and then allocation of the photosynthetic fixed carbon to lipid, carbohydrate and protein take place all within a cell. In green algae, starch (as main storage carbohydrates) synthesis and *de novo* fatty acid synthesis mainly take place in plastid [63], while TAG assembly seems to occur in plastid and endoplasmic reticulum (ER) [3]. In our model for *N. oceanica*, TAG synthesis was likely in plastid and ER [24], while the degradation of storage carbohydrates seems to occur in cytoplasm (Fig. 8). Thus in *N. oceanica* the cytoplasm may function as the "source tissue" while plastid and ER as the "sink tissue" for carbon partitioning, whereas certain yet-to-defined transporting systems may function as the "phloem".

For microalgae, so far very few reports on mechanisms of carbon partitioning have been available [62,64,65]. We have previously shown that in *C. reinhardtii* starch synthesis is linked to TAG synthesis [11,13]. Distinct from *C. reinhardtii*, *N. oceanica* produces β-1,3-glucan but not starch as storage carbohydrates [24,62]. Furthermore *Nannochloropsis* spp. produce PC whereas *C. reinhardtii* does not, thus redirection of carbon flow from PC to TAG only takes place in *N. oceanica* but not in *C. reinhardtii* [62]. Thus the carbon partitioning models of oleaginous microalgae can be highly distinct from laboratory model microalgae, and further research is required to reveal the diversity and evolution of such models in microalgae.

This *N. oceanica* carbon partitioning model can guide genetic engineering for enhanced TAG productivity, as biosynthesis of storage carbohydrates and neutral lipids in microalgae may compete for the same sources of carbon precursors (e.g., glucose, acetyl–CoA, and reducing power). Here the observed transient accumulation of polymeric glucose and continuous accumulation of free glucose under N− implied that the β-1,3-glucan may serve as a temporary carbon storage form.

Biosynthesis of β-1,3-glucans was found to be transcriptionally regulated, and thus down-regulation or blocking of these genes (e.g. *BGT* and *BS*) by gene knockdown or gene knockout should reduce the accumulation of β-1,3-glucan and shunt the carbon flow to the competing pathways that include TAG biosynthesis. Furthermore, "pulling" glucose from storage carbohydrates into the glycolysis pathway may represent another strategy for increasing the carbon flow into TAG biosynthesis. One key here is to "pull" carbon intermediates towards synthesis of acetyl–CoA, the precursor of fatty acid biosynthesis, otherwise the accumulated carbon intermediates (e.g. UDP-glucose, fructose-6-P) can be utilized for biosynthesis of the other two major sugars, e.g. galactose and mannitol. *PDH* genes can be a promising candidate to "pull" carbon intermediates into TAG biosynthesis, since they showed remarkable up-regulation under N− (Fig. 7).

In addition to the conversion of carbohydrates into the precursors for TAG biosynthesis, recycling of acyl-groups from membrane lipids represents another redirection of carbon flux leading to TAG accumulation in response to stresses. PDAT is a sole enzyme in an acyl-CoA-independent TAG biosynthesis, but its physiological role is poorly defined [22,66,67]. In both yeasts and plant leaves, PDAT activities were linked to the exponential growth phase cells whereas they were less prominent in the stationary growth phase yeast cells and the senescing leaves [68,69]. In *Arabidopsis*, PDAT was primarily involved in the deacylation–reacylation cycle of membrane lipid turnover in vigorously growing cells, which implied the dependence of membrane lipid turnover on *de novo* fatty acid biosynthesis [69]. In *C. reinhardtii*, the PDAT-mediated membrane lipid turnover for TAG biosynthesis was not only crucial for exponential growth phase cells but also was accelerated by N deprivation [22]. In *N. oceanica* IMET1, *PDAT* transcripts reached the highest level at the early stage following N deprivation, while during the same period, carbon flow into the *de novo* biosynthesis of glycerolipid (including both membrane and storage lipids) was elevated. In this scenario, the membrane lipids synthesized in the plastid (e.g. MGDG and DGDG) or those associated with the plastid envelope membranes (e.g. PC) may serve as a buffer system to reserve a portion of fatty acids that cannot be immediately utilized by either the PDAT-based acyl-CoA-dependent TAG biosynthesis or β-oxidation.

Lipases may also contribute to the reallocation of carbon from membrane lipids to TAG synthesis. In *C. reinhardtii* under N deprivation, transcripts of lipase genes were among the most drastically fluctuated among all lipid-related genes, with most of them up-regulated [34]. In *N. oceanica* IMET1 under N−, the patatin-like lipase gene *PPP* (g4525) showed remarkable up-regulation, indicative of its possible involvement in fatty acyl fluxing from membrane lipids to TAG. Patatin-like phospholipases constituted a major family of acyl-hydrolyzing lipases in *Arabidopsis* [70]. An *Arabidopsis* patatin-like phospholipase gene *pPLAIIIδ* highly expressed in developing embryos was found to play a role in PC acyl remodeling for TAG biosynthesis [71]. Characterization of this IMET1 patatin-like phospholipase should help to define its role in TAG biosynthesis and may help in exploiting it for controlling carbon partitioning.

5. Conclusion

In *N. oceanica*, we demonstrated the presence of eight monosaccharides (glucose, galactose, mannitol, fucose, rhamnose, mannose, ribose and glucosamine) in IMET1, with the first three as the major components. Under N+, lamilarin may be the major storage carbon; it serves as a temporary carbon storage and likely competes for carbon sources with TAG. Under N−, the up-regulation of β-1,3-glucan metabolic pathways along with *PDH* mediated acetyl–CoA synthesis and membrane lipid turnover/degradation contributed to the augmented TAG synthesis. These findings have implications in genetic engineering for the enhancement of oil production in this and related microalgae.

Acknowledgments

This work was funded by the Ministry of Science and Technology of China (2012CB721101 and 2012AA02A707), the International Research Collaboration Program (31010103907) and the Young Investigator Program (61103167) from National Natural Science Foundation of China and Initiative from Chinese Academy of Sciences. We thank Wei Chen (Institute of Hydrobiology, Chinese Academy of Sciences) for assistance in analysis of total lipid and total carbohydrate content and Jordan Pacheco (Arizona State University) for assistance in GC-FID based fatty-acid composition analysis.

Appendix A. Supplementary data

Supplementary data to this article can be found online at http://dx.doi.org/10.1016/j.algal.2014.11.005.

References

[1] Y. Chisti, Biodiesel from microalgae, Biotechnol. Adv. 25 (2007) 294–306.
[2] Q. Hu, M. Sommerfeld, E. Jarvis, et al., Microalgal triacylglycerols as feedstocks for biofuel production: perspectives and advances, Plant J. 54 (2008) 621.
[3] S.S. Merchant, J. Kropat, B. Liu, et al., TAG, you're it! Chlamydomonas as a reference organism for understanding algal triacylglycerol accumulation, Curr. Opin. Biotechnol. 23 (2012) 352–363.
[4] R.H. Wijffels, M.J. Barbosa, An outlook on microalgal biofuels, Science 329 (2010) 796–799.
[5] D.R. Georgianna, S.P. Mayfield, Exploiting diversity and synthetic biology for the production of algal biofuels, Nature 488 (2012) 329–335.
[6] A. Beattie, E.L. Hirst, E. Percival, Studies on the metabolism of the Chrysophyceae. Comparative structural investigations on leucosin (chrysolaminarin) separated from diatoms and laminarin from the brown algae, Biochem. J. 79 (1961) 531–537.
[7] M.T. Guarnieri, A. Nag, S.L. Smolinski, et al., Examination of triacylglycerol biosynthetic pathways via *de novo* transcriptomic and proteomic analyses in an unsequenced microalga, PLoS One 6 (2011) e25851.
[8] J.P. Ral, C. Colleoni, F. Wattebled, et al., Circadian clock regulation of starch metabolism establishes GBSSI as a major contributor to amylopectin synthesis in *Chlamydomonas reinhardtii*, Plant Physiol. 142 (2006) 305–317.
[9] J. Ohlrogge, J. Browse, Lipid biosynthesis, Plant Cell 7 (1995) 957–970.
[10] G. Michel, T. Tonon, D. Scornet, et al., Central and storage carbon metabolism of the brown alga *Ectocarpus siliculosus*: insights into the origin and evolution of storage carbohydrates in Eukaryotes, New Phytol. 188 (2010) 67–81.
[11] Y. Li, D. Han, G. Hu, et al., *Chlamydomonas* starchless mutant defective in ADP-glucose pyrophosphorylase hyper-accumulates triacylglycerol, Metab. Eng. 12 (2010) 387–391.
[12] V.H. Work, R. Radakovits, R.E. Jinkerson, et al., Increased lipid accumulation in the *Chlamydomonas reinhardtii sta7-10* starchless isoamylase mutant and increased carbohydrate synthesis in complemented strains, Eukaryot. Cell 9 (2010) 1251–1261.
[13] Y. Li, D. Han, G. Hu, et al., Inhibition of starch synthesis results in overproduction of lipids in *Chlamydomonas reinhardtii*, Biotechnol. Bioeng. 107 (2010) 258–268.
[14] Z. Wang, N. Ullrich, S. Joo, et al., Algal lipid bodies: stress induction, purification, and biochemical characterization in wild-type and starchless *Chlamydomonas reinhardtii*, Eukaryot. Cell 8 (2009) 1856.
[15] I.K. Blaby, A.G. Glaesener, T. Mettler, et al., Systems-level analysis of nitrogen starvation-induced modifications of carbon metabolism in a *Chlamydomonas reinhardtii* starchless mutant, Plant Cell 25 (2013) 4305–4323.
[16] J. Sheehan, T. Dunahay, R. Benemann, et al., A look back at the U.S. department of energy's Aquatic species Program: biodiesel from algae, Close-out Report, National Renewable Energy Laboratory, Department of Energy, Golden, CO, 1998.
[17] F. Daboussi, S. Leduc, A. Maréchal, et al., Genome engineering empowers the diatom *Phaeodactylum tricornutum* for biotechnology, Nat. Commun. 5 (2014).
[18] G.Q. Chen, Y. Jiang, F. Chen, Fatty acid and lipid class composition of the eicosapentaenoic acid-producing microalga, *Nitzschia laevis*, Food Chem. 104 (2007) 1580–1585.
[19] G. Chen, Y. Jiang, F. Chen, Salt-induced alterations in lipid composition of diatom *Nitzschia laevis* (Bacillariophyceae) under heterotrophic culture condition, J. Phycol. 44 (2008) 1309–1314.
[20] J. Harwood, Membrane lipids in algae, in: S. Paul-André, M. Norio (Eds.), Lipids in Photosynthesis: Structure, Function and Genetics, Springer, Netherlands, Dublin, 1998, pp. 53–64.
[21] X. Li, Eric R. Moellering, B. Liu, et al., A galactoglycerolipid lipase is required for triacylglycerol accumulation and survival following nitrogen deprivation in *Chlamydomonas reinhardtii*, Plant Cell 24 (2012) 4670–4686.
[22] K. Yoon, D. Han, Y. Li, et al., Phospholipid:diacylglycerol acyltransferase is a multifunctional enzyme involved in membrane lipid turnover and degradation while synthesizing triacylglycerol in the unicellular green microalga *Chlamydomonas reinhardtii*, Plant Cell 24 (2012) 3708–3724.
[23] D. Simionato, M.A. Block, N. La Rocca, et al., The response of *Nannochloropsis gaditana* to nitrogen starvation includes *de novo* biosynthesis of triacylglycerols, a decrease of chloroplast galactolipids, and reorganization of the photosynthetic apparatus, Eukaryot. Cell 12 (2013) 665–676.

[24] J. Li, D. Han, D. Wang, et al., Choreography of transcriptomes and lipidomes of *Nannochloropsis* reveals the mechanisms of oil synthesis in microalgae, Plant Cell (2014), http://dx.doi.org/10.1105/tpc.1113.121418.
[25] Y. Xiao, J. Zhang, J. Cui, et al., Metabolic profiles of *Nannochloropsis oceanica* IMET1 under nitrogen-deficiency stress, Bioresour. Technol. 130 (2013) 731–738.
[26] A. Sukenik, Ecophysiological considerations in the optimization of eicosapentaenoic acid production by Nannochloropsis sp. (Eustigmatophyceae), Bioresour. Technol. 35 (1991) 263–269.
[27] D. Wang, Y. Lu, H. Huang, et al., Establishing oleaginous microalgae research models for consolidated bioprocessing of solar energy, in: F.-W. Bai, C.-G. Liu, H. Huang, G.T. Tsao (Eds.), Biotechnology in China III: Biofuels and Bioenergy, Springer, Berlin Heidelberg, 2012, pp. 69–84.
[28] C.E. Carpinelli, A. Telatin, N. Vitulo, et al., Chromosome scale genome assembly and transcriptome profiling of *Nannochloropsis gaditana* in nitrogen depletion, Mol. Plant 7 (2014) 323–335.
[29] R. Radakovits, R.E. Jinkerson, S.I. Fuerstenberg, et al., Draft genome sequence and genetic transformation of the oleaginous alga *Nannochloropis gaditana*, Nat. Commun. 3 (2012) 686.
[30] K. Pan, J. Qin, S. Li, et al., Nuclear monoploidy and asexual propagation of *Nannochloropsis oceanica* (Eustigmatophyceae) as revealed by its genome sequence, J. Phycol. 47 (2011) 1425–1432.
[31] A. Vieler, G. Wu, C.-H. Tsai, et al., Genome, functional gene annotation, and nuclear transformation of the heterokont oleaginous alga *Nannochloropsis oceanica* CCMP1779, PLoS Genet. 8 (2012) e1003064.
[32] L. Wei, Y. Xin, D. Wang, et al., Nannochloropsis plastid and mitochondrial phylogenomes reveal organelle diversification mechanism and intragenus phylotyping strategy in microalgae, BMC Genomics 14 (2013) 534.
[33] D. Wang, K. Ning, J. Li, et al., *Nannochloropsis* genomes reveal evolution of microalgal oleaginous traits, PLoS Genet. 10 (2014) e1004094.
[34] R. Miller, G. Wu, R.R. Deshpande, et al., Changes in transcript abundance in *Chlamydomonas reinhardtii* following nitrogen deprivation predict diversion of metabolism, Plant Physiol. 154 (2010) 1737–1752.
[35] H. Dong, E. Williams, D. Wang, et al., Responses of *Nannochloropsis oceanica* IMET1 to long-term nitrogen starvation and recovery, Plant Physiol. 162 (2013) 1110–1126.
[36] M. DuBois, K.A. Gilles, J.K. Hamilton, et al., Colorimetric method for determination of sugars and related substances, Anal. Chem. 28 (1956) 350–356.
[37] J.A. Berges, A.E. Fisher, P.J. Harrison, A comparison of Lowry, Bradford and Smith protein assays using different protein standards and protein isolated from the marine diatom *Thalassiosira pseudonana*, Mar. Biol. 115 (1993) 187–193.
[38] Y. Li, M. Sommerfeld, F. Chen, et al., Consumption of oxygen by astaxanthin biosynthesis: a protective mechanism against oxidative stress in *Haematococcus pluvialis* (Chlorophyceae), J. Plant Physiol. 165 (2008) 1783–1797.
[39] T. Govender, L. Ramanna, I. Rawat, et al., BODIPY staining, an alternative to the Nile Red fluorescence method for the evaluation of intracellular lipids in microalgae, Bioresour. Technol. 114 (2012) 507–511.
[40] L.L. Laurens, M. Quinn, S. Wychen, et al., Accurate and reliable quantification of total microalgal fuel potential as fatty acid methyl esters by in situ transesterification, Anal. Bioanal. Chem. 403 (2012) 167–178.
[41] W.W. Christie, X. Han, Chapter 7 — preparation of derivatives of fatty acids, in: W.W. Christie, X. Han (Eds.), Lipid Analysis, Woodhead Publishing, Cambridge, 2012, pp. 145–158.
[42] J.K. Volkman, M.R. Brown, G.A. Dunstan, et al., The biochemical composition of marine microalgae from the class Eustigmatophyceae1, J. Phycol. 29 (1993) 69–78.
[43] S.A. Scott, M.P. Davey, J.S. Dennis, et al., Biodiesel from algae: challenges and prospects, Curr. Opin. Biotechnol. 21 (2010) 277–286.
[44] W.R. Riekhof, C. Benning, Chapter 2 — glycerolipid biosynthesis, in: E.H. Harris, D.B. Stern, G.B. Witman (Eds.), The Chlamydomonas Sourcebook, Academic Press, London, 2009, pp. 41–68.
[45] A. Aloulou, Y. Ali, S. Bezzine, et al., Phospholipases: an overview, in: G. Sandoval (Ed.), Lipases and Phospholipases, Humana Press, Totowa, 2012, pp. 63–85.
[46] Y. Jia, F. Tao, W. Li, Lipid profiling demonstrates that suppressing *Arabidopsis* phospholipase Dδ retards ABA-promoted leaf senescence by attenuating lipid degradation, PLoS One 8 (2013) e65687.
[47] D.J. Oliver, B.J. Nikolau, E.S. Wurtele, Acetyl-CoA—life at the metabolic nexus, Plant Sci. 176 (2009) 597–601.
[48] B. Gschloessl, Y. Guermeur, J.M. Cock, HECTAR: a method to predict subcellular targeting in heterokonts, BMC Bioinforma. 9 (2008) 393.
[49] M.G. Claros, MitoProt, a Macintosh application for studying mitochondrial proteins, Comput. Appl. Biosci. 11 (1995) 441–447.
[50] T.N. Petersen, S. Brunak, G. von Heijne, et al., SignalP 4.0: discriminating signal peptides from transmembrane regions, Nat. Methods 8 (2011) 785–786.
[51] O. Emanuelsson, H. Nielsen, G.V. Heijne, ChloroP, a neural network-based method for predicting chloroplast transit peptides and their cleavage sites, Protein Sci. 8 (1999) 978–984.
[52] K. Iwamoto, Y. Shiraiwa, Salt-regulated mannitol metabolism in algae, Mar. Biotechnol. 7 (2005) 407–415.
[53] A. Groisillier, Z. Shao, G. Michel, et al., Mannitol metabolism in brown algae involves a new phosphatase family, J. Exp. Bot. 65 (2013) 559–570.
[54] P. Kroth, A. Chiovitti, A. Gruber, et al., A model for carbohydrate metabolism in the diatom *Phaeodactylum tricornutum* deduced from comparative whole genome analysis, PLoS One 3 (2008).
[55] A. Melis, Carbon partitioning in photosynthesis, Curr. Opin. Chem. Biol. 17 (2013) 453–456.
[56] A. Lacointe, Carbon allocation among tree organs: a review of basic processes and representation in functional-structural tree models, Ann. For. Sci. 57 (2000) 521–533.
[57] P.E.H. Minchin, M.R. Thorpe, What determines carbon partitioning between competing sinks? J. Exp. Bot. 47 (1996) 1293–1296.
[58] T.H. Nielsen, B. Veierskov, Regulation of carbon partitioning in source and sink leaf parts in sweet pepper (*Capsicum annuum* L.) plants, Plant Physiol. 93 (1990) 637–641.
[59] D.M. Braun, T.L. Slewinski, Genetic control of carbon partitioning in grasses: roles of sucrose transporters and Tie-dyed loci in phloem loading, Plant Physiol. 149 (2009) 71–81.
[60] J. Pozueta Romero, P. Perata, T. Akazawa, Sucrose-starch conversion in heterotrophic tissues of plants, Crit. Rev. Plant Sci. 18 (1999) 489–525.
[61] E. Baroja Fernandez, E. Etxeberria, F.J. Munoz, et al., An important pool of sucrose linked to starch biosynthesis is taken up by endocytosis in heterotrophic cells, Plant Cell Physiol. 47 (2006) 447–456.
[62] U. Klein, Intracellular carbon partitioning in *Chlamydomonas reinhardtii*, Plant Physiol. 85 (1987) 892–897.
[63] M.V. Busi, J. Barchiesi, M. Martín, et al., Starch metabolism in green algae, Starch-Stärke 66 (2014) 28–40.
[64] D.H. Turpin, F.C. Botha, R.G. Smith, et al., Regulation of carbon partitioning to respiration during dark ammonium assimilation by the green alga *Selenastrum minutum*, Plant Physiol. 93 (1990) 166–175.
[65] X. Johnson, J. Alric, Central carbon metabolism and electron transport in *Chlamydomonas reinhardtii*: metabolic constraints for carbon partitioning between oil and starch, Eukaryot. Cell 12 (2013) 776–793.
[66] A. Dahlqvist, U. Ståhl, M. Lenman, et al., Phospholipid:diacylglycerol acyltransferase: an enzyme that catalyzes the acyl-CoA-independent formation of triacylglycerol in yeast and plants, Proc. Natl. Acad. Sci. U. S. A. 97 (2000) 6487–6492.
[67] H. Zhang, H.G. Damude, N.S. Yadav, Three diacylglycerol acyltransferases contribute to oil biosynthesis and normal growth in *Yarrowia lipolytica*, Yeast 29 (2012) 25–38.
[68] P. Oelkers, A. Tinkelenberg, N. Erdeniz, et al., A lecithin cholesterol acyltransferase-like gene mediates diacylglycerol esterification in yeast, J. Biol. Chem. 275 (2000) 15609–15612.
[69] J. Fan, C. Yan, X. Zhang, et al., Dual role for phospholipid:diacylglycerol acyltransferase: enhancing fatty acid synthesis and diverting fatty acids from membrane lipids to triacylglycerol in *Arabidopsis* leaves, Plant Cell 25 (2013) 3506–3518.
[70] M. Li, S.C. Bahn, L. Guo, et al., Patatin-related phospholipase pPLAIIIbeta-induced changes in lipid metabolism alter cellulose content and cell elongation in Arabidopsis, Plant Cell 23 (2011) 1107–1123.
[71] M. Li, S.C. Bahn, C. Fan, et al., Patatin-related phospholipase pPLAIIIdelta increases seed oil content with long-chain fatty acids in Arabidopsis, Plant Physiol. 162 (2013) 39–51.